Shell closure effects in the stable $^{74-82}$Se isotopes from magnetic moment measurements using projectile excitation and the transient field technique

K.-H. Speidel,[1] N. Benczer-Koller,[2] G. Kumbartzki,[2] C. Barton,[3] A. Gelberg,[4] J. Holden,[2] G. Jakob,[5,*] N. Matt,[2] R. H. Mayer,[2] M. Satteson,[2] R. Tanczyn,[6,†] and L. Weissman[7]

[1]*Institut für Strahlen und Kernphysik, Universität Bonn, Bonn, Germany*

[2]*Department of Physics and Astronomy, Rutgers University, New Brunswick, New Jersey 08903*

[3]*Department of Physics, Clark University, Worcester, Massachusetts 01610*

[4]*Institut für Kernphysik, Universität zu Köln, Germany*

[5]*Physik-Department der Technischen Universität München, Germany*

[6]*Department of Physical Science, Kutztown University, Kutztown, Pennsylvania 19530*

[7]*Weizmann Institute of Science, Rehovot, Israel*

(Received 1 December 1997)

Projectile excitation and the transient field technique have been used to measure the g factors of the 2_1^+, 2_2^+, and 4_1^+ states in $^{74-82}$Se in order to study the influence of the $N=50$ shell closure at low excitation energies. The states of interest were populated by Coulomb exciting beams of the appropriate isotope by the same natural Si target. The results demonstrate that inverse kinematics provides a very powerful technique, highly suitable for measurements with radioactive beams. The g factors obtained for $^{74-82}$Se are compared with results from IBM-II calculations. [S0556-2813(98)02005-6]

PACS number(s): 21.10.Ky, 25.70.De, 27.50.+e

I. INTRODUCTION

The stable $^{74-82}$Se isotopes are transitional nuclei displaying some unexpected features. Besides a varying collectivity reflected by the $B(E2)$ values, they exhibit pronounced single-particle and shell effects. Figure 1 displays the main decay features of low-lying states of these isotopes while Table I shows the available data on branching ratios, lifetimes, and $B(E2)$'s of the 2_1^+, 0_2^+, 2_2^+, and 4_1^+ states. The Se isotopes do not behave either like good vibrators or good rotors. The ratio $E(4^+)/E(2^+)$ increases from 2.1 to 2.7 across the sequence of isotopes while the branching ratio $I(2_2^+ \rightarrow 2_1^+)/I(2_2^+ \rightarrow 0_1^+)$ varies from 0.3 to 2.0. The $B(E2)$'s for the transitions from the 2_1^+, 0_2^+, 2_2^+, and 4_1^+ states indicate some collectivity, but not an overwhelming contribution. Kaup and collaborators [1] have carried out, within the interacting boson model (IBM-II), systematic calculations for Kr, Sr, and Se isotopes to determine the extent to which single-particle excitations compete with collective degrees of freedom.

Over the last 20 years, magnetic moments of short-lived nuclear states have been measured by the transient field technique. In its conventional application, target nuclei are excited by heavy ion beams and are simultaneously ejected from the target material with high velocity. These fast ions then traverse a ferromagnetic material such as iron or gadolinium in which they interact with the polarized electrons. The net effect of this interaction is an effective hyperfine interaction at the nucleus which results in a precession of the angular distribution of decay γ rays. This angular precession is directly proportional to the magnetic moment of the excited state under study.

In the experiment described below it is the beam that is Coulomb excited by a target nucleus whereas the target remains the same for all different beams to be studied. Coulomb excitation of ^{80,82}Se beams was first applied by Kavka *et al.* [2]. However, Speidel and collaborators [3] first used the inverse reaction kinematics method for g-factor measurements. The technique has the advantage of keeping all experimental conditions fairly constant, and thus allows for ready comparison of different nuclei interacting with the same target. It provides high efficiency for detection of the reaction products and high velocity of the recoiling ions, features which are essential attributes for transient field measurements. It has the added advantage of being the only method available for the study of magnetic moments of radioactive nuclei for which no stable target exists. These ex-

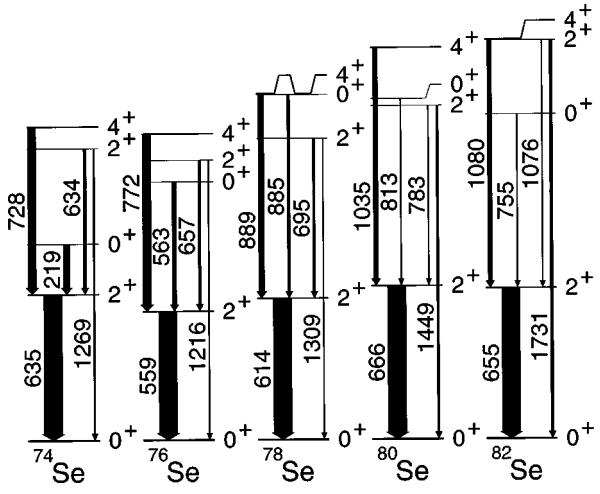

FIG. 1. Low-lying states in $^{74-82}$Se.

*Present address: Department of Physics and Astronomy, Rutgers University, New Brunswick, NJ 08903.

†Deceased.

TABLE I. Spectroscopic data on the low-lying levels of $^{74-82}$Se [22]. Energies are in MeV, mean lives in ps, $B(E2)$'s in e^2 fm^4 or in Weisskopf units (second line), and $B(M1)$'s in μ_N^2.

	^{74}Se	^{76}Se	^{78}Se	^{80}Se	^{82}Se
$E(2_1^+)$	0.6348	0.5591	0.6137	0.6662	0.6547
$\tau(2_1^+)$	10.2(1)	17.7(3)	14.0(4)	12.4(2)	18.9(3)
$E(0_2^+)$	0.8538	1.1223	1.4986	1.4792	1.4099
$\tau(0_2^+)$	1080(72)	16(7)	2.6(4)	16.4(25)	43.3
$E(2_2^+)$	1.2690	1.2610	1.3086	1.4492	1.7313
$\tau(2_2^+)$	5.8(16)	4.9(3)	6.1(4)	2.81(10)	1.36(16)
$E(4_1^+)$	1.3632	1.3308	1.5028	1.7012	1.7351
$\tau(4_1^+)$	2.68(12)	2.19(7)	1.51(7)	0.95(3)	1.38(22)
$E(4_1^+)$/E(2_1^+)	2.147	2.38	2.449	2.553	2.650
$I(2_2^+\rightarrow 2_1^+)$/I$(2_2^+\rightarrow 0_1^+)$	1.96	1.69	1.33	0.68	0.30
$\delta(2_2^+)$	$-5.6(16)$	$+5.2(2)$	$+3.5(5)$	$-5.0(^{+2}_{-6})$	
$B(E2;\ 2_1^+\rightarrow 0_1^+)$	775(10)	844(14)	670(19)	504(8)	359(6)
	41.3(5)	43.5(7)	33.3(9)	24.2(4)	16.7(3)
$B(E2;\ 0_2^+\rightarrow 2_1^+)$	1500(100)	906(396)	578(89)	140(21)	77
	80(5)	46.6(204)	28.7(44)	6.7(10)	3.6
$B(E2;\ 4_1^+\rightarrow 2_1^+)$	1485(66)	1361(44)	973(45)	722(23)	402(64)
	79.2(35)	70.1(23)	48.4(22)	34.7(11)	18.7(30)
$B(E2;\ 2_2^+\rightarrow 2_1^+)$	884(244)	823(50)	439(29)	384(14)	96(11)
	47.1(130)	42.4(26)	21.8(14)	18.5(7)	4.5(5)
$B(M1;\ 2_2^+\rightarrow 2_1^+)$	0.00072(54)			0.00071(53)	
$B(E2;\ 2_2^+\rightarrow 0_1^+)$	15(4)	23(1)	15(1)	27(1)	29(3)
	0.8(2)	1.2(1)	0.7(1)	1.3(1)	1.3(1)

periments are thus precursors of similar types of study with radioactive beams which are being planned at a variety of facilities around the world.

II. EXPERIMENTAL TECHNIQUE

The experimental details for measuring magnetic moments of short-lived excited states by the transient field technique have been described in previous publications [3,4]. In the current experiments, isotopic beams of $^{74-82}$Se between 230 and 262 MeV were accelerated by the Wright Nuclear Science Laboratory Tandem at Yale. All five Se isotopes were produced from a natural Se cone in the UNIS source. Figure 2 shows the intensity profile of the beam at the entrance to the accelerator.

The target was a composite of several materials. A layer of 0.95 mg/cm^2 of natural Si was evaporated on a 4.4 mg/cm^2 gadolinium substrate which was itself evaporated on a 1.0 mg/cm^2 tantalum foil backed by 1.35 mg/cm^2 of aluminum [5]. In addition, a 7.5 mg/cm^2 copper foil was placed behind the target to stop the beam. The target and beam stop were mounted on the tip of a closed cycle refrigerator which

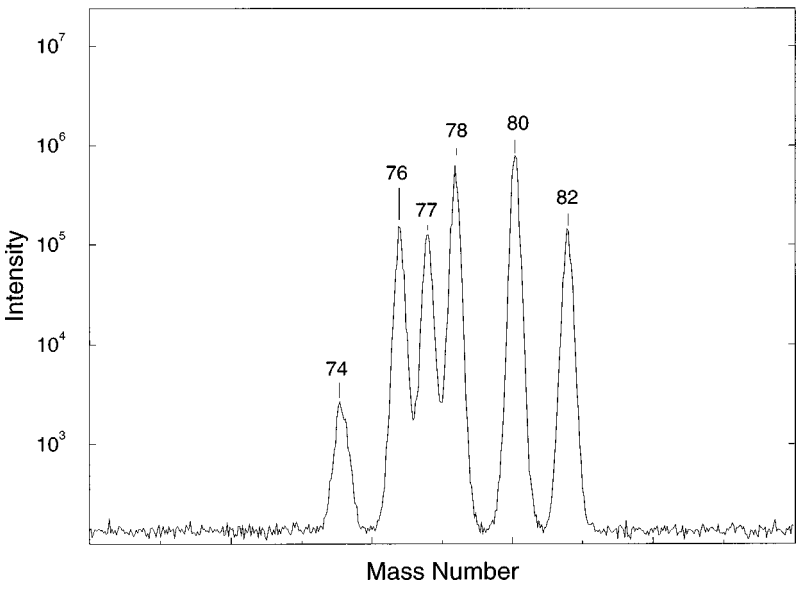

FIG. 2. Spectrum of ions emitted by the ion source at the WNSL Tandem accelerator.

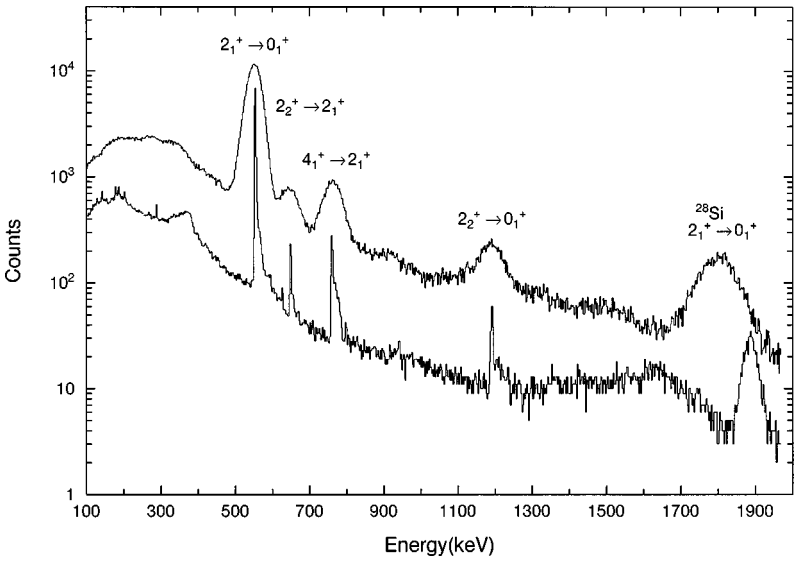

FIG. 3. Spectrum of ^{76}Se γ rays in coincidence with ^{28}Si ions. While the upper curve shows the spectrum obtained with a NaI(Tl) detector the curve below shows the spectrum obtained with a Ge detector. As can be seen from the Ge spectrum there are no additional γ lines contaminating any of the transitions analyzed. Since the Ge detector was placed at the forward angle of 10° with respect to the beam axis, the fully Doppler-shifted γ line from the $(2_1^+ \rightarrow 0_1^+)$ transition in ^{28}Si occurs at a higher energy in comparison to the spectrum taken with the NaI(Tl) detector placed at 65°.

was operated at a temperature of 50 K during the run.

The magnetization of the target was measured, before and after each experiment, as a function of temperature from 11 K to 300 K in an ac magnetometer [6]. The magnetization was constant over a temperature range from 44 K to 122 K. During the experiment, an external magnetic field was applied to the target to magnetize the gadolinium foil. In the experiments carried out at beam energies of 230 MeV, the external magnetic field was 0.04 T which resulted in a target magnetization of $M(50\ \mathrm{K})=0.1746$ T. For the experiments at other energies, a lower external field was used, 0.03 T, resulting in a smaller target magnetization, $M(50\ \mathrm{K})=0.1641$ T.

The excited beam nuclei traverse the ferromagnetic layer and stop in the cubic environment free of further electronic interactions. The recoiling H-like Si ions had enough velocity to emerge from the beam stop and were detected by a 100-μm-thick passivated implanted planar silicon detector placed at 0° subtending an angle of $\pm 13°$.

The γ rays in coincidence with forward-scattered ^{28}Si ions were detected in four 12.7 cm $\times$ 12.7 cm NaI(Tl) detectors located at a distance of 17.5 cm from the target. A Ge detector was placed at a forward angle of 10° to the beam axis to monitor through γ-ray line shapes the adherence of target layers and to ensure that no impurity radiations contributed to the background under the γ-ray lines. The data were recorded in event mode. Typical coincidence spectra measured with NaI(Tl) and Ge detectors are shown in Fig. 3. The γ rays deexciting the 2_1^+, 4_1^+, and 2_2^+ states are clearly identified and resolved. In addition, a Doppler-shifted γ ray corresponding to the $(2_1^+ \rightarrow 0_1^+)$ transition from forward-scattered ^{28}Si ions which were Coulomb excited to their first 2^+ state by the beam ions is also observed.

Angular correlations of the emitted γ rays were determined from the measured anisotropy ratios of coincident γ rays at 45° and 90°. For the measurement of precessions the detectors were placed at complementary angles $\theta_0 = \pm 65°$ and $\pm 115°$ with respect to the beam direction. Beam-bending effects in the fringe field of the magnet were found to be negligible because of effective shielding.

Two sets of experiments were carried out. In the first, all $^{74-82}$Se isotopes were accelerated to 230 MeV. In the second, the beam energy was varied in order to maintain the same kinematic profile for the excited Se ions traversing the gadolinium layer. In this case energies of 262, 253, and 236 MeV, respectively, were used for beams of ^{74}Se, ^{76}Se, and ^{80}Se. The average entrance and exit energies and velocities for the excited Se ions in the gadolinium layer are displayed in Table II.

III. DATA ANALYSIS AND RESULTS

The measured precession effect ϵ for the radiation deexciting a certain state can be expressed as

$$\epsilon = \frac{\rho - 1}{\rho + 1}, \tag{1}$$

where $\rho = (\rho_{14}/\rho_{23})$ is determined from the double ratios

$$\rho_{ij} = \sqrt{\frac{N_i^{\uparrow}/N_i^{\downarrow}}{N_j^{\uparrow}/N_j^{\downarrow}}}, \tag{2}$$

and the coefficients $i = 1,2$ and $j = 3,4$ represent the four detectors; $N_{i,j}^{\uparrow}$ and $N_{i,j}^{\downarrow}$ are the coincidence counting rates of

TABLE II. Characteristics of the reaction kinematics. $\langle E_{\mathrm{in}} \rangle$, $\langle E_{\mathrm{out}} \rangle$, $\langle v/v_0 \rangle_{\mathrm{in}}$, and $\langle v/v_0 \rangle_{\mathrm{out}}$ are, respectively, the average energies and velocities of the ^{A}Se isotopes as they enter into and exit from the gadolinium foil. $v_0 = e^2/\hbar$ is the Bohr velocity.

	Beam energy (MeV)	$\langle E_{\mathrm{in}} \rangle$ (MeV)	$\langle E_{\mathrm{out}} \rangle$ (MeV)	$\langle v/v_0 \rangle_{\mathrm{in}}$	$\langle v/v_0 \rangle_{\mathrm{out}}$
^{74}Se	230	35.5	3.25	4.40	1.33
	262	39.1	3.48	4.61	1.45
^{76}Se	230	36.5	3.57	4.40	1.38
	253	39.5	4.10	4.58	1.40
^{78}Se	230	37.4	3.90	4.40	1.42
^{80}Se	230	38.2	4.21	4.39	1.46
	236	39.6	4.48	4.47	1.50
^{82}Se	230	39.4	4.63	4.40	1.51
^{28}Si[a]	230–262			15.0	14.0

[a]Target excitation.

TABLE III. Calculated Coulomb excitation cross sections for the 2_1^+, 0_2^+, 2_2^+, and 4_1^+ states in the ^{A}Se isotopes at the indicated beam energies and for Si particles detected between 0° and 13°.

	Beam energy (MeV)	$\sigma(2_1^+)$ (10^{-2} b)	$\sigma(0_2^+)$ (10^{-2} b)	$\sigma(2_2^+)$ (10^{-2} b)	$\sigma(4_1^+)$ (10^{-2} b)
^{74}Se	230	1.483	0.321	0.190	0.394
	262	1.117	0.449	0.280	0.584
^{76}Se	230	2.005	0.179	0.226	0.431
	253	1.706	0.253	0.311	0.618
^{78}Se	230	2.222	0.072	0.112	0.254
^{80}Se	230	2.019	0.017	0.107	0.144
	236	1.990	0.014	0.095	0.122
^{82}Se	230	1.832	0.007	0.044	0.053

the photopeak of the γ transition in the ith or jth detector with the external field pointing ''up'' ($\uparrow$) and ''down'' ($\downarrow$) with respect to the plane of the reaction. The γ-ray photopeak intensities have been corrected for random and background rates. Similar ''cross ratios'' $\rho_c=(\rho_{24}/\rho_{13})$ and ϵ_c were calculated to check for systematic effects that might mask the true precession. In all cases, vanishingly small ϵ_c were obtained. The precession angles $\Delta\theta$ are derived from the measured ϵ's through the relationship

$$\Delta\theta=\epsilon/S, \tag{3}$$

where S is the logarithmic slope $S(\theta_0)=(1/W)(dW/d\theta)$ of the angular correlation at the angles of interest θ_0.

The substate alignment parameter $w(m=0)$ was derived from a fit of the anisotropy ratios to the predictions of angular correlation theory [7]. The populations of the 2_1^+ states from either direct excitation or feeding from the 0_2^+, 2_2^+, and 4_1^+ states were obtained from Coulomb excitation calculations and the known spectroscopic parameters (Table I). The total cross sections for Coulomb excitation of the 2_1^+, 0_2^+, 2_2^+, and 4_1^+ states under the experimental conditions of this experiment were calculated on the basis of the Winther–de Boer COULEX code and are displayed in Table III.

A substate alignment of $w(m=0)=0.95$ was obtained for all isotopes and energies except for ^{74}Se at 262 MeV which is close to the Coulomb barrier. A lower alignment, $w(m=0)=0.88$, fits the data best, yielding slightly lower slopes. It should be emphasized that for the higher beam energies the possibility of non-Coulomb excitation reactions have been considered but no appreciable effects were observed. In fact the angular correlation population parameters $w(m=0)$ were well accounted for by assuming only Coulomb excitation. A summary of all logarithmic slopes is found in Table IV.

The determination of the precession angle $\Delta\theta$ for the 2_2^+ and 4_1^+ states follows directly from Eq. (3). However, the determination of the precession angle $\Delta\theta$ for the first 2^+ states requires a more elaborate analysis due to significant contributions from feeding from the 0_2^+, 2_2^+, and the 4_1^+ states. This feeding affects the precession in two ways: (i) the *slope* of the measured $(2_1^+\rightarrow 0_1^+)$ angular correlation is a composite of contributions from the feeding states, and (ii) the *precessions* of the 4_1^+ and 2_2^+ states themselves (the 0_2^+ state does not precess) must be taken into account explicitly. Both these effects are characterized by the population strength of the feeding states and by the angular correlations in which the feeding transitions to the 2_1^+ state are not observed. Additional terms have to be included in the analysis due to the fact that, in ^{74}Se, the feeding $(2_2^+\rightarrow 2_1^+)$ transition has almost the same energy as the $(2_1^+\rightarrow 0_1^+)$ transition, and similarly in ^{76}Se, the $(0_2^+\rightarrow 2_1^+)$ is not resolved from the $(2_1^+\rightarrow 0_1^+)$ transition.

The measured ϵ's of the 2_1^+ states can be expressed as [8]

$$\epsilon_{2_1^+}^{\text{meas}}=\frac{\Sigma_i \epsilon_i S_i(\theta_0) P_i W_i(\theta_0)}{\Sigma_i S_i(\theta_0) P_i W_i(\theta_0)}, \tag{4}$$

where ϵ_i, $S_i(\theta_0)$, P_i, and $W_i(\theta_0)$ refer to the ϵ values of the feeding states. S_i and W_i are the slopes and correlation functions at θ_0 of the ith transition and P_i the population strength of the feeding states proportional to the total Coulomb excitation cross section (Table III). Similarly, the average slope $\langle S\rangle$ which is directly related to the measured angular correlation can be expressed as [8]

$$S^{\text{meas}}\equiv\langle S\rangle=\frac{\Sigma_i S_i(\theta_0) P_i W_i(\theta_0)}{\Sigma_i P_i W_i(\theta_0)}. \tag{5}$$

The $\Delta\theta(2_1^+)$ can now be derived from the known $S_i(\theta_0), P_i, W_i(\theta_0)$, and the ϵ's of the 2_1^+, 4_1^+, and 2_2^+ states. The results are summarized in Table V.

TABLE IV. Summary of logarithmic slopes of the angular correlations at ± 65° or ± 115° derived from the measured anisotropies A and angular correlation theory [7]. The average logarithmic slope $\langle S(2_1^+\rightarrow 0_1^+)\rangle$ is a weighted average of the slopes of the direct excitation of the 2_1^+ state and the slope components arising from feeding from the 0_2^+, 2_2^+, and 4_1^+ states (see text). Errors quoted refer to those measured for the anisotropies A.

	^{74}Se		^{76}Se		^{78}Se	^{80}Se		^{82}Se
E (MeV)	230	262	230	253	230	230	236	230
$A(2_1^+;45°/90°)$		2.35(5)		3.31(6)	5.19(3)	6.47(4)	6.05(7)	
$\langle S(2_1^+\rightarrow 0_1^+)\rangle$	1.96	1.46(3)	2.27	1.93(2)	2.40(1)	2.58(1)	2.53(1)	2.63
$S(4_1^+\rightarrow 2_1^+)$	1.08	1.05	1.08		1.08	1.08		1.08
$S(2_2^+\rightarrow 0_1^+)$	2.68	2.44	2.68		2.68	2.68		2.68
$S(2_2^+\rightarrow 2_1^+)$	0.35	0.30	0.30		0.35	0.30		0.34

TABLE V. Measured precessions for transitions observed in the decays of the 2_1^+, 2_2^+, and 4_1^+ states in the $^{74-82}$Se isotopes. The γ-ray detectors were placed at $\pm 65°$ and $\pm 115°$ with respect to the beam.

	Beam Energy (MeV)	$-\Delta\theta(2_1^+ \rightarrow 0_1^+)$ (mrad)	$-\Delta\theta(2_2^+ \rightarrow 0_1^+)$ (mrad)	$-\Delta\theta(4_1^+ \rightarrow 2_1^+)$ (mrad)
^{74}Se	230	19.53(60)	22.4(39)	17.7(38)
	262	15.5(26)	28.8(97)	23.6(80)
^{76}Se	230	18.82(40)	14.1(33)	21.8(34)
	253	16.4 (15)	14.0(41)	28.9(77)
^{78}Se	230	17.85(44)	14.9(47)	17.5(52)
^{80}Se	230	19.91(35)	13.7(45)	17.4(73)
	236	16.47(56)	11.3(59)	13.6(130)
^{82}Se	230	23.30(33)		17.8(119)

Finally, the g factors could be determined from the expression

$$\Delta\theta = -g\frac{\mu_N}{\hbar}\int_{t_{\rm in}}^{t_{\rm out}} B(v(t),Z)e^{-t/\tau}dt, \qquad (6)$$

where B, the transient field, is a function of the velocity v and atomic number Z of the probe ion, τ is the mean lifetime of the state being examined, and $t_{\rm in}$ and $t_{\rm out}$ are the mean entrance and exit times of the ions into or out of the ferromagnet. However, in order to obtain results independent of the magnetization of the gadolinium layer and uncertainties inherent in existing parametrizations of the transient field, g factors were obtained from the measured precessions $\Delta\theta$ by calibrating the field with the known g factor of ^{82}Se(2_1^+), $g = 0.496(29)$. This value had been determined previously using the transient field technique with a ^{32}S beam [9]. It is noted that the calibration procedure used in the current experiment avoids the problem arising from possible deterioration of the target magnetization induced by the ion beam with subsequent reduction of the effective transient field [10] because all measurements were performed with similar beam intensities and for Se ions with the same stopping powers in gadolinium. Nevertheless, a distinct difference in the precession of the ^{80}Se(2_1^+) state was observed in the two runs at comparable beam energies of 230 MeV and 236 MeV (Table V). This difference was attributed to different intrinsic target magnetizations during the two experiments. This observation was made possible only by the high precision of the measured precessions of the 2_1^+ state. The effect was not visible in the precessions of the 2_2^+ and 4_1^+ states because of the lower accuracy of the measurement (Table V). Hence the precessions measured in the different experiments were normalized through the measured precession of the ^{80}Se(2_1^+) state which was experimentally determined at both 230 MeV and 236 MeV.

The effect of the beam on the magnetization is particularly pronounced in the precession of the ^{28}Si(2_1^+) state which was measured simultaneously. The measured precession $\Delta\theta = -2.7(8)$ mrad implies a transient field attenuation for ^{28}Si ions of $\simeq 0.3$ which is in good agreement with earlier observations and systematic measurements on H-like ions relevant to the present beam-target conditions. It is noted that this attenuation, however, is substantially weaker for the Se ions [10].

IV. RESULTS

The technique of inverse kinematics coupled with Coulomb excitation of the beam allowed measurements of the g factors of the 2_1^+ states of all stable $^{74-82}$Se isotopes with a relative accuracy of the order of 1–2 %; the g factors of the 2_2^+ and 4_1^+ states were measured for the first time.

The absolute g factors of individual excited states were derived from the measured precession angles $\Delta\theta$. The precession angles were corrected for the differences in the kinematics encountered by ions of different masses traversing the gadolinium foils. Both the Rutgers [11] and the linear [12] parametrizations of the transient field have been used to determine these corrections, yielding the same results.

The results are displayed in Fig. 4 as ratios of $g(^A\text{Se}(2_1^+))$ to $g(^{74}\text{Se}(2_1^+))$, the g factor of the lightest isotope in the series. These g factor ratios are insensitive to uncertainties in the transient field parametrizations. The magnetic moment of the 2_1^+ state of ^{82}Se had been measured by the transient field technique in both iron and gadolinium environments, yielding $g = 0.481(38)$ and 0.516(45), respectively [9]. The average of these values, $g = 0.496(29)$, is adopted as the reference with respect to which the absolute g factors of the other isotopes are determined even though an earlier measurement by the ion implantation perturbed angular correlation technique had yielded a smaller value, $g = 0.43(12)$ [13]. However, in order to minimize systematic errors due to the different techniques, the transient field value was adopted in this paper. The agreement between the previous transient field experiments and the present results is very good. The absolute values of the g factors are displayed in Table VI.

V. DISCUSSION

The magnetic moments of the 2_1^+ states have been measured with higher accuracy than any others in this region and therefore can provide a stringent test of the nuclear models. It is evident from the data that while the measured magnetic moments are of the order of the Z/A prediction for collective models, they also exhibit marked structure as a function of neutron numbers.

The present results are discussed in the framework of the proton-neutron IBM-II which should be applicable to the even-even Se nuclei in view of their transitional character. The atomic number $Z = 34$ is far from the closed shell num-

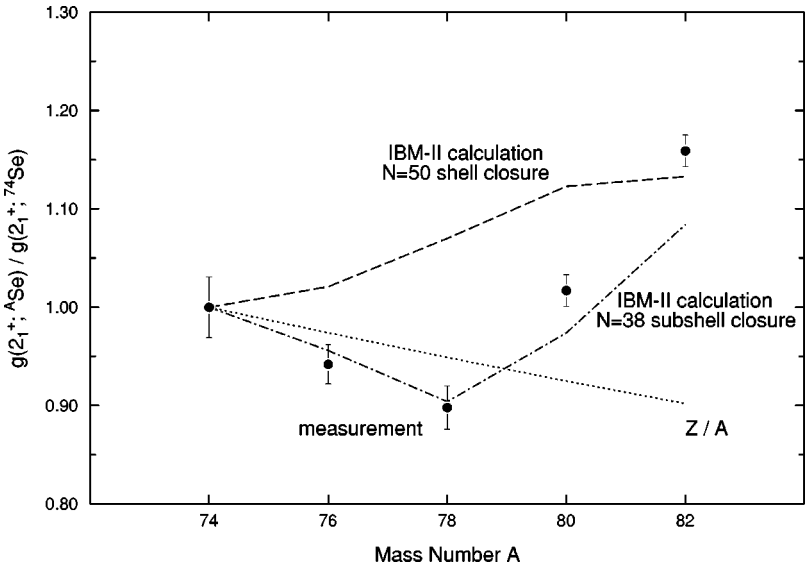

FIG. 4. Ratio of measured $g(^{A}\mathrm{Se}(2_1^+))$ to $g(^{74}\mathrm{Se}(2_1^+))$ in comparison with the IBM-II calculations. The dashed curve shows the results for the calculations dealing with $N=50$ ($N_\nu^{\max}=5$ for ^{74}Se and $N_\nu^{\min}=1$ for ^{82}Se) as shell closure whereas the dashed-dot curve assumes an additional subshell closure at $N=38$ (besides the $N=50$ closure) with $N_\nu^{\max}=3$ for ^{78}Se and $N_\nu^{\min}=1$ for ^{74}Se as well as ^{82}Se. The dip in the g factor ratio can only be explained for the latter case.

ber $Z=28$. The neutron number varies from 48 in the case of ^{82}Se, near shell closure at $N=50$, to 40 (^{74}Se), significantly far from 50, but approaching a possible additional subshell closure at $N=40$, observed at $Z=40$ in the Zr region.

Extensive calculations had been carried out in the past [1,14] to explain several properties of these nuclei in a consistent way. Kaup *et al.* [1] calculated low excitation energies and $E2$ matrix elements within the IBM-II and obtained results in good agreement with observed level energies and the $E2$ transition probabilities. However, they did not predict $B(M1)$'s or g factors. Radhi and Stewart [14] did calculate the g factors of the 2_1^+ states in $^{72-80}$Se within the IBM-II, but did not discuss the implications of their results because of the large uncertainties in the experimental values available at the time. Their results, a constant $g=0.40$ for $^{74-78}$Se and a slightly larger $g=0.43$ for ^{80}Se, do not agree with the present much more accurate data. In addition, the new g factors of the 2_2^+ and 4_1^+ states have not yet been discussed within the IBM-II. Therefore, new calculations based on slightly different input parameters were necessary in order to obtain a better agreement with the magnetic properties of these nuclei and reproduce simultaneously the experimental electric quadrupole moments and transition probabilities.

Throughout the present calculations, which are based on the work by Otsuka *et al.* [15], the code NPBOS described in Ref. [16] was applied. The Hamiltonian

$$H=(\varepsilon_d+\varepsilon_{d_\pi})n_{d_\pi}+(\varepsilon_d+\varepsilon_{d_\nu})n_{d_\nu}+\kappa Q_\pi\cdot Q_\nu+aM, \quad (7)$$

where ε_d denotes the binding energy for the d bosons and ε_{d_π} and ε_{d_ν} are the deviations from this value for the proton and neutron d bosons, respectively, was used. The proton (neutron) quadrupole operators $Q_{\pi,\nu}$ containing the deformation parameters $\chi_{\pi,\nu}$ are connected to each other by the parameter κ, and M denotes the Majorana interaction operator with the strength parameter a. The parameters used are identical to those of Kaup *et al.* [1] with the exception of $\chi_\pi=-0.35$ and $a=0$ (instead of $\chi_\pi=-0.9$ and $a=0.1$ in [1]) and the nonvanishing values for ε_{d_π}, ε_{d_ν} ($\varepsilon_{d_\pi}=\varepsilon_{d_\nu}=0$ in [1]). If the input parameters of Ref. [1] are used, the calculated $B(M1)$'s become about two orders of magnitude larger than the experimental ones. In addition, the unusual boson g factors [14]

$$g_\pi=0.7 \quad \text{and} \quad g_\nu=0.2,$$

TABLE VI. Comparison of the experimental g factors of the 2_1^+, 4_1^+, and 2_2^+ states in $^{74-82}$Se and the theoretical values deduced from IBM-II calculations for shell closure at $N=50$. The measured g factor quoted for the 2_1^+ of ^{82}Se is the average of the values obtained in Ref. [9] with iron and gadolinium hosts. The errors in the g factors reflect both the statistical errors of the current measurements and the error in the calibration value $g(^{82}\mathrm{Se}(2_1^+))$ (see text). The errors in the ratios of g factors represent only the statistical errors in the measured precessions (see Table V). The input data for the IBM-II calculations are given in Table VII.

	$g(2_1^+)$		$g(4_1^+)$		$g(2_2^+)$		$\frac{g(2_1^+;\,^{A}\mathrm{Se})}{g(2_1^+;\,^{74}\mathrm{Se})}$		Z/A
	Expt.	Calc.	Expt.	Calc.	Expt.	Calc.	Expt.	Calc.	
^{74}Se	0.428(27)	0.383	0.50(10)	0.368	0.55(9)	0.360	1.000(31)	1.000	0.459
^{76}Se	0.403(23)	0.391	0.64(9)	0.381	0.35(6)	0.373	0.942(20)	1.021	0.447
^{78}Se	0.384(25)	0.410	0.39(12)	0.408	0.33(11)	0.408	0.898(22)	1.070	0.436
^{80}Se	0.435(27)	0.430	0.68(25)	0.447	0.35(10)	0.465	1.017(16)	1.123	0.425
^{82}Se	0.496(29) [a]	0.434	0.57(38)	0.553	–	0.508	1.159(16)	1.133	0.415

[a]Reference [9].

which substantially deviate from the standard values [17,18]

$$g_\pi \gtrsim 1 \quad \text{and} \quad g_\nu \lesssim 0,$$

had to be used to reproduce both experimental $B(M1)$'s and g factors. More standard boson g factors can be used together with other a values to explain the data. However, since no information on mixed symmetry 2^+ states exists as yet, there is no way to fit the Majorana parameter to experimental data. Therefore the parameter a was set to zero.

In contrast to the work of Ref. [14] where small variations of g_π, g_ν, and the Majorana interaction were allowed for different isotopes, these parameters were kept constant for all isotopes throughout the present calculations. The magnetic dipole operator in the IBM-II can be written as [17]

$$T(M1,\mu) = \sqrt{\frac{3}{4\pi}}\left(\frac{1}{2}(g_\pi + g_\nu)L^{(1)}_\mu + \frac{1}{2}(g_\pi - g_\nu) \times (L^{(1)}_{\pi,\mu} - L^{(1)}_{\nu,\mu})\right), \tag{8}$$

with

$$L^{(1)}_{\rho,\mu} = \sqrt{10}(d^\dagger_\rho \tilde{d}_\rho)^{(1)}_\mu, \quad \rho = \pi,\nu,$$

where the first term of the magnetic dipole operator $T(M1,\mu)$ represents the total angular momentum operator $L^{(1)}_\mu = L^{(1)}_{\pi,\mu} + L^{(1)}_{\nu,\mu}$ and is diagonal. Therefore, only the second term of Eq. (8) gives a contribution to the $B(M1)$'s. The $B(M1)$'s, consequently, show a strong dependence on both the absolute difference of the deformation parameters $|\chi_\pi - \chi_\nu|$, which are contained in the $L^{(1)}_{\rho,\mu}$ ($\rho = \pi,\nu$) operators, and the magnetic moments $|g_\pi - g_\nu|$. In this context it should be noted that, within the IBM-II, $M1$ transitions between low-lying collective states are only allowed if these states contain components with less than maximum F spin [18]. The magnitude of this so-called F-spin breaking is mainly determined by the magnitude of $|\chi_\pi - \chi_\nu|$ [19].

The lower collective states are usually characterized by the maximum F-spin value $F_{\max} = (N_\pi + N_\nu)/2$ where $N_{\pi,\nu}$ are the proton and neutron boson numbers, respectively. For the Se nuclei $N_\pi = 3$ and N_ν varies from $N_\nu = 5$ in ^{74}Se ($N = 40$) to $N_\nu = 1$ in ^{82}Se ($N = 48$). If the states are totally symmetric with respect to both boson species, that is, if F spin is conserved, the g factor is given by

$$g = g_\pi \frac{N_\pi}{N_\pi + N_\nu} + g_\nu \frac{N_\nu}{N_\pi + N_\nu}, \tag{9}$$

which can be expressed in terms of F spin as

$$g = \frac{g_\pi + g_\nu}{2} + \frac{g_\pi - g_\nu}{2}\frac{F_0}{F_{\max}}, \tag{10}$$

where the first term is the F-spin scalar, the second term is the F-spin vector part, and

$$\frac{F_0}{F_{\max}} = \frac{N_\pi - N_\nu}{N_\pi + N_\nu}.$$

TABLE VII. Values of proton, neutron boson numbers, and IBM-II parameters used as input into the Hamiltonian of Eq. (7) for $^{74-82}$Se. ε_d, ε_{d_π}, ε_{d_ν}, and κ are given in units of MeV; all other parameters have no dimensions. Most parameters have been adopted from Ref. [1] with the exception of $\chi_\pi = -0.35$ and the Majorana parameter $a = 0$ instead of $\chi_\pi = -0.9$ and $a = 0.1$ in [1]. In addition, the d boson binding energies have been set different for protons and neutrons. However, the sum energy of all d bosons as well as the sum of $(\chi_\pi + \chi_\nu)$ has not been changed for any of these isotopes from the corresponding values in Ref. [1]. $e_\pi = e_\nu = 0.08$ e b and $g_\pi = 0.7$, $g_\nu = 0.2$ for all isotopes.

A	74	76	78	80	82
N_π	3	3	3	3	3
N_ν	5	4	3	2	1
ε_d	1.05	0.96	0.99	0.98	0.96
ε_{d_π}	0.10	0.10	0.10	0.10	0.10
ε_{d_ν}	−0.06	−0.075	−0.10	−0.15	−0.30
κ	−0.13	−0.16	−0.21	−0.24	−0.26
χ_π	−0.35	−0.35	−0.35	−0.35	−0.35
χ_ν	−0.27	−0.055	0.16	0.375	0.55

The g factors obtained for the various excited states using the set of input parameters shown in Table VII are summarized and compared to the experimental results in Table VI. As can also be seen in Fig. 4 the calculations suggest a monotonic increase in the g factors as a function of N and do not explain the observed drop at $N = 42,44$.

If one assumes an additional subshell closure at $N = 38$ (besides $N = 50$) and the neutron boson numbers are renumbered accordingly, the model predicts g factor ratios in fairly good agreement with the experimental values (Fig. 4). However, neither the $B(E2)$'s nor the level energies, especially for ^{74}Se, could be reproduced simultaneously with $N_\nu = 1$ instead of $N_\nu = 5$ and with the Hamiltonian given by Eq. (7). Hence, a more comprehensive Hamiltonian such as that used by Radhi and Stewart [14] was used. This Hamiltonian includes additional terms for the d-boson conserving residual neutron-neutron and proton-proton interaction of the form [16]

$$V_{\rho\rho} = \frac{1}{2}c^\rho_L (d^\dagger_\rho \times d^\dagger_\rho)^{(L)} \cdot (\tilde{d}_\rho \times \tilde{d}_\rho)^{(L)}, \quad \rho = \pi,\nu, \tag{11}$$

as well as the Majorana operator containing the parameters ξ_1, ξ_2, ξ_3 which provide different interaction strengths for d bosons coupling to the angular momenta $L = 1,2,3$. In order to reproduce the electric properties [$B(E2)$'s and quadrupole moments] of ^{74}Se and ^{76}Se with reduced boson numbers, the boson charges of both protons and neutrons had to be increased to $e_\pi = 0.12$ e b and $e_\nu = 0.10$ e b over the previously adopted $e_\pi = e_\nu = 0.08$ e b. In addition, the absolute value of the quadrupole-quadrupole interaction κ was varied over values between -0.20 MeV and -0.30 MeV and both quadrupole deformation parameters χ_π and χ_ν had to be set to ≈ -1 to compensate for the decreased $E2$ transition strengths. This calculation yields results in better agreement

with the data (Fig. 4). However, it is not clear that the assumption of a subshell closure at $N=38$ is physical.

A conceivable subshell closure at $N=40$, as has been suggested for $Z=40$ [20], is ruled out by the calculations, as $M1$ transitions would be forbidden in the model for ^{74}Se, contrary to observations [21]. In addition, the g factors for all states in ^{74}Se would become $g=g_\pi\sim 0.7$, which does not agree with the measured value $g(2_1^+)=0.428(27)$ (Table VI). Further experimental corroboration of these assumptions is necessary.

In summary, ratios of magnetic moments of the 2_1^+, 2_2^+, and 4_1^+ states in $^{74-82}$Se have been measured with the highest accuracy available to date using the transient field method following Coulomb excitation of the beam in inverse kinematics. The accuracies of the absolute g factors are determined mainly from the value of the $g(2_1^+)$ factor of ^{82}Se.

ACKNOWLEDGMENTS

One of us (K.-H. S.) wishes to thank the Rutgers Nuclear Physics Laboratory for hosting summer visits in 1996–1997. The authors wish to thank Dr. P. Maier-Komor (Physik-Department der Technischen Universität München) for preparing the target and T. Otsuka (University of Tokyo) for advice and discussions on the IBM-II calculations. We also are thankful to the accelerator staff of the Wright Nuclear Structure Laboratory for their support. This work was supported in part by the U.S. National Science Foundation.

[1] U. Kaup, C. Mönkemeyer, and P. v. Brentano, Z. Phys. A **310**, 129 (1983).
[2] A. E. Kavka, C. Fahlander, A. Bäcklin, D. Cline, T. Czosnyka, R. M. Diamond, D. Disdier, W. J. Kernan, L. Kraus, I. Linck, N. Schulz, J. Srebrny, F. S. Stephens, L. E. Svensson, B. Varnestig, E. G. Vogt, and C. Y. Wu, Nucl. Phys. **A593**, 177 (1995).
[3] K.-H. Speidel, J. Cub, U. Reuter-Knopp, W. Karle, H. Busch, S. Kremeyer, J. Gerber, and F. Hagelberg, Z. Phys. A **342**, 17 (1992).
[4] N. Benczer-Koller, M. Hass, and J. Sak, Annu. Rev. Nucl. Sci. **30**, 53 (1980).
[5] P. Maier-Komor, Nucl. Instrum. Methods Phys. Res. A **282**, 131 (1989).
[6] A. Piqué, J. M. Brennan, R. Darling, R. Tanczyn, D. Ballon, and N. Benczer-Koller, Nucl. Instrum. Methods Phys. Res. A **279**, 579 (1989).
[7] H. J. Rose and D. M. Brink, Rev. Mod. Phys. **39**, 306 (1967).
[8] D. Ballon, Y. Niv, S. Vajda, N. Benczer-Koller, L. Zamick, and G. A. Leander, Phys. Rev. C **33**, 1461 (1986).
[9] M. Brennan, N. Benczer-Koller, M. Hass, and H. T. King, Hyperfine Interact. **4**, 268 (1978).
[10] G. Jakob, J. Cub, K.-H. Speidel, S. Kremeyer, H. Busch, U. Grabowy, A. Gohla, O. Jessensky, and J. Gerber, Z. Phys. D **32**, 7 (1994).
[11] N. K. B. Shu, D. Melnik, J. M. Brennan, W. Semmler, and N. Benczer-Koller, Phys. Rev. C **21**, 1828 (1980).
[12] K.-H. Speidel, G. Jakob, U. Grabowy, J. Cub, S. Kremeyer, H. Busch, A. Gohla, O. Jessensky, J. Gerber, and A. Méens, Phys. Lett. B **324**, 130 (1994).
[13] G. M. Heestand, R. R. Borchers, B. Herskind, L. Grodzins, R. Kalish, and D. E. Murnick, Nucl. Phys. **A133**, 310 (1969).
[14] F. S. Radhi and N. M. Stewart, Z. Phys. A **356**, 145 (1996).
[15] T. Otsuka, A. Arima, and F. Iachello, Nucl. Phys. **A309**, 1 (1978).
[16] T. Otsuka and N. Yoshida, computer program NPBOS, Japan Atomic Energy and Research Institute Report No. JAERI-M85-094, 1985.
[17] M. Sambataro, O. Scholten, A. E. L. Dieperink, and G. Piccitto, Nucl. Phys. **A423**, 333 (1984).
[18] K.-H. Kim, A. Gelberg, T. Mizusaki, T. Otsuka, and P. v. Brentano, Nucl. Phys. **A604**, 163 (1996).
[19] P. O. Lipas, P. v. Brentano, and A. Gelberg, Rep. Prog. Phys. **53**, 1335 (1990), and references therein.
[20] A. Wolf, D. D. Warner, and N. Benczer-Koller, Phys. Lett. **158B**, 7 (1985).
[21] Nucl. Data Sheets **74**, 529 (1995).
[22] R. B. Firestone and V. S. Shirley, *Table of Isotopes* (Wiley, New York, 1996).